

| |
|-------------------------|
| I.D. # |
| Name Philip Phillips |
| Subject Physics 560 |
| Course Section |
| Instructor |
| Date |

Receiving or giving aid in a final examination is a cause for dismissal from the University.

(Begin Writing on this page)

Lecture 10:

1.) Review: We proved last time the Hohenberg-Kohn theorem: The density uniquely defines the ground state energy of an electronic system. The simplest D.F.T. is that of Thomas-Fermi.

$$\text{Kinetic energy: } T[n] = V \left(\frac{d^3}{(2\pi)^3} \frac{\hbar^2 k^2}{2m} \right) = \frac{3}{5} V \frac{\hbar^2}{2m} (3\pi^2)^{2/3} n^{5/3}.$$

$$\text{Exchange: } E_{\text{exch}} \propto n^{4/3}.$$

$$\text{direct: } \frac{1}{2} \int dr dr' \frac{n(r) n(r')}{|r-r'|}.$$

$$\Rightarrow E[n] = \frac{\hbar^2}{2m} \frac{3}{5} (3\pi^2)^{2/3} \int dr n^{5/3} + \int dr n(r) U(r)$$

$$+ \frac{1}{2} \int dr_1 dr_2 \frac{n(r_1) n(r_2)}{|r_1 - r_2|} - \frac{3}{4} \left(\frac{3}{\pi} \right)^{1/3} e^2 \int dr n^{4/3}.$$

$$\Rightarrow \mu = \frac{\delta E}{\delta n} = \frac{\hbar^2}{2m} (3\pi^2)^{2/3} n^{2/3} + U(r) + e^2 \int \frac{n(r')}{|r-r'|} dr' - \left(\frac{3}{\pi} \right)^{1/3} e^2 n^{1/3}$$

In the 1980's, J. Schwinger derived systematic corrections to T.F. theory. I heard him give a colloq. at Berkeley about it in 1983: A tour de force. Check out: arXiv:1907.0475 for the highlights.

2.) Stability of Matter:

Why don't electrons collapse into a nucleus? The K.E. scales as $\hbar^2/2ma^2$ while the Pot. energy $-e^2/a$. Let's apply Heisenberg to

$$\frac{\hbar^2}{2ma^2} - \frac{e^2}{a} = E; \quad \frac{\partial E}{\partial a} \Big|_{a_0} = 0 = -\frac{\hbar^2}{ma_0^3} + \frac{e^2}{a_0^2} \Rightarrow a_0 = \hbar^2/me^2 \quad \uparrow \text{Bohr radius.}$$

$$E = \frac{\hbar^2}{2m} \left(\frac{me^2}{\hbar^2} \right)^2 - e^2 \frac{me^2}{\hbar^2} = \frac{me^4}{2\hbar^2} = \frac{e^2}{2a_0} = 13.6 \text{ eV.}$$

So let's use Heisenberg's inequality.

$$\left[\int dr \hbar^2 |\nabla \psi|^2 \right] \left[\int dr r^2 |\psi|^2 \right] \geq \frac{\hbar^2}{4}.$$

$$\Rightarrow T[N] \geq \hbar^2/8m \int dr n(r) r^2.$$

Leib showed that

$$T[N] \geq \frac{\hbar^2}{2m} \frac{9.116}{(8\pi)^{2/3}} \int dr n^{5/3}$$

which accounts for the stability of matter.

3.) Cohesion of Solids:

We will treat a.) ionic crystals and b.) metals.

a.) Ionic Crystals:

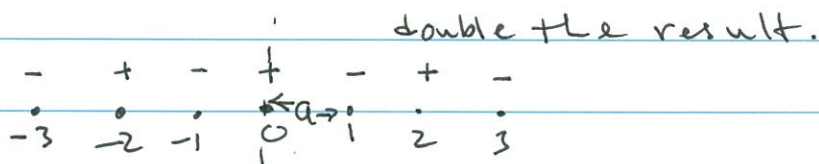
How are such crystals NaCl stable. $\text{Na} \rightarrow \text{Na}^+$ Ion
 $\text{Cl} \rightarrow \text{Cl}^- = E_A$ (electron affinity). Generally,
 $I > E_A$. So why are ionic crystals stable?

Here's the answer: Coulomb interaction.

$$I - E_A + E_M < 0. \quad E_M = \text{Madelung energy.}$$

$$E_M = \sum_{i,j} \frac{z_i z_j}{|r_i - r_j|}$$

Consider a 1-d crystal:



$$r_{ij} = a|i-j|$$

$$\Rightarrow E_M = \frac{e^2}{a} N \sum_{i,j} \frac{(\pm)_{ij}}{|i-j|}$$

\swarrow
 N identical
 terms.

$$\Rightarrow E_M = \frac{2Ne^2}{a} \left(-\frac{1}{1} + \frac{1}{2} - \frac{1}{3} + \frac{1}{4} - \dots \right)$$

$$= -\frac{2e^2 N}{a} \left(1 - \frac{1}{2} + \frac{1}{3} - \frac{1}{4} + \dots \right)$$

$$= -\frac{2e^2 N}{a} \sum_{l=0}^{\infty} \frac{(-1)^l}{1+l} = -2e^2 N \sum_{l=1}^{\infty} \frac{(-1)^{l-1}}{l}$$

$$= -\frac{2e^2 N}{a} \ln 2.$$

In general E_M depends on the lattice structure.

$$E_M = -\frac{e^2 N}{a} \alpha$$

For a bcc lattice $\alpha = 1.76268$

fcc $\alpha = 1.74757$

Cohesive Energy of Metals

see 6.3 of Phillips

non-interacting value of ϵ_F^0 well approximates the experimentally observed bandwidth. At the Hartree–Fock level, the bandwidth expands to

$$\Delta = \epsilon_F^0(1 + 0.331r_s). \quad (6.23)$$

The increase in the bandwidth, $\sim 0.331r_s$, is illustrated in Fig. 6.1(b).

6.3 Cohesive energy of metals

One of the key problems to which the Hartree–Fock approximation has been applied is the cohesive energy of a metal. When free atoms are brought together to form a metal, their energy decreases. The cohesive energy is defined as the difference

$$\epsilon_{\text{coh}} = (\epsilon/\text{atom})_{\text{metal}} - (\epsilon/\text{atom})_{\text{free atom}},$$

and it is negative in a bound metal. The measured cohesive energies in the alkalis are:

| eV | Li | Na | K | Rb | Cs |
|-------------------------------|-------|-------|-------|-------|--------|
| $\epsilon_{\text{coh, expt}}$ | -1.58 | -1.13 | -0.98 | -0.82 | -0.815 |

In order to calculate cohesive energies quantitatively, two improvements beyond Hartree–Fock need to be made. In addition to describing better the correlations among electrons, it is necessary to go beyond the approximation that the ions form a uniform background and take into account more precisely the interaction of the electrons with the ions and the average Coulomb energy of the ions. We follow here the strategy of Wigner and Seitz (WS1933) to calculate the cohesive energy of a metal, a scheme that enabled them to carry out the first quantitative application of quantum mechanics to calculating realistic properties of solids.

6.3.1 Wigner–Seitz method

The main idea of the Wigner–Seitz method is to divide the crystal into (Wigner–Seitz) cells, each containing a single ion and Z electrons, and to treat the interactions within each cell reasonably accurately. Since each cell is electrically neutral, the interaction energy between cells can be ignored to a first approximation. The cohesive energy is then given by

$$\epsilon_{\text{coh}} = \epsilon_0 - \epsilon_{\text{atom}} + \epsilon_{\text{kin}} + \epsilon_{\text{coul}}, \quad (6.24)$$

where ϵ_0 is the lowest energy of a conduction electron in the cell, physically the energy of the bottom of the conduction band, ϵ_{kin} is the average electron kinetic energy, and ϵ_{coul} is the average electron–electron Coulomb energy.

At this point, we restrict our attention to the alkali metals, in which a single conduction electron and an ion reside in each cell. One can initially ignore electron–electron interactions within each cell. Most simply, the Wigner–Seitz cell can be taken to be a sphere about the ion. To calculate ϵ_0 , we solve the Schrödinger equation

$$\left(\frac{\hat{p}^2}{2m} + V_{\text{ion}} \right) \varphi_0(\mathbf{r}) = \epsilon_0 \varphi_0(\mathbf{r}) \quad (6.25)$$

for the lowest conduction electron level in the presence of the ion potential. The boundary condition at the edge of each cell is that the normal derivative $\varphi'_0(r) = 0$.

The resulting ϵ_0 s are shown in Table 6.2.

| Table 6.2 | | | | | |
|---------------------------------------|-------|-------|-------|-------|-------|
| eV | Li | Na | K | Rb | Cs |
| ϵ_{atom} | -5.37 | -5.16 | -4.34 | -4.17 | -3.89 |
| ϵ_0 | -9.15 | -8.25 | -6.58 | -6.18 | -5.85 |
| $\epsilon_0 - \epsilon_{\text{atom}}$ | -3.78 | -3.09 | -2.24 | -2.01 | -1.95 |

As is evident, $\epsilon_0 - \epsilon_{\text{atom}} < 0$, resulting from interactions between neighboring ions in a crystal that delocalize the electrons, an effect which ultimately lowers their energy.

The simplest estimate of ϵ_0 assumes that the ion provides a central $1/r$ potential and that, as a consequence of the exclusion principle with the core electrons, the electron cannot get closer than a_0 to the central potential. Consequently,

$$\epsilon_0 \simeq -n_e \int_{a_0}^{r_s} dr \frac{e^2}{r} \quad (6.26)$$

$$= -\frac{3e^2}{2r_s^3} (r_s^2 - a_0^2) = -\frac{40.82 \text{ eV}}{r_s} \left(1 - \frac{1}{r_s^2} \right). \quad (6.27)$$

We next include the kinetic energy of the conduction electrons. The kinetic energy per electron in a free gas is given by

$$\epsilon_{\text{kin}}^0 = \frac{3}{5} \frac{p_F^2}{2m} = \frac{2.21}{r_s^2} \text{ Ry}. \quad (6.28)$$

Here is a list of r_s values and corresponding kinetic energies for the alkalis:

| Table 6.3 | | | | | |
|-------------------------|------|------|------|------|------|
| eV | Li | Na | K | Rb | Cs |
| r_s | 3.22 | 3.96 | 4.87 | 5.18 | 5.57 |
| ϵ_{kin} | 2.90 | 1.92 | 1.26 | 1.12 | 0.97 |

To set the scale, we ignore Coulomb interactions and compute the cohesive energy from just ϵ_0 , Eq. (6.27), and the kinetic energy as $\epsilon_{\text{coh}} \approx \epsilon_0 - \epsilon_{\text{atom}} + \epsilon_{\text{kin}}$, and find:

Table 6.4

| eV | Li | Na | K | Rb | Cs |
|------------------------------|-------|-------|-------|-------|--------|
| $\epsilon_{\text{coh,NI}}$ | -0.89 | -1.17 | -0.97 | -0.89 | -0.98 |
| $\epsilon_{\text{coh,expt}}$ | -1.58 | -1.13 | -0.98 | -0.82 | -0.815 |

As is evident, our estimates of the cohesive energy at this level of theory are in fair to poor agreement with experiment.

We now include the direct Coulomb energy, treating the electron density as uniform and replacing each cell by a sphere of radius r_e . In such a sphere, the number of electrons enclosed in a sphere of radius $r < r_e$ is $n(r) = 4\pi r^3 n_e / 3$. The direct Coulomb energy is

$$\epsilon_{\text{direct}} = \int_0^{r_e} dr \frac{e^2}{r} n_e n(r). \quad (6.29)$$

Evaluating the integral, we obtain

$$\epsilon_{\text{direct}} = \frac{3}{5} \frac{e^2}{r_e} = \frac{6}{5r_s} \text{Ry}. \quad (6.30)$$

The interaction energy between neutral Wigner-Seitz cells is a higher order correction, which can be included in a more precise calculation.

We next include the exchange Coulomb energy at the Hartree-Fock level, assuming again that the electron density is uniform. From Eq. (6.15), the exchange energy is

$$\epsilon_{\text{exch}} = -\frac{0.916}{r_s} \text{Ry}. \quad (6.31)$$

The total electron-electron Coulomb energy is then

$$\epsilon_{\text{coul}} = \epsilon_{\text{exch}} + \epsilon_{\text{direct}} = \frac{0.284}{r_s} \text{Ry}, \quad (6.32)$$

and the cohesive energy becomes

$$\epsilon_{\text{coh,HF}} = \epsilon_0 - \epsilon_{\text{atom}} + \epsilon_{\text{kin}} + \epsilon_{\text{coul}}. \quad (6.33)$$

The Coulomb energy, together with a comparison of the new cohesive energies with the experimental values (P1955), is shown below:

Table 6.5

| eV | Li | Na | K | Rb | Cs |
|------------------------------|-------|-------|-------|-------|-------|
| ϵ_{coul} | 1.24 | 1.01 | 0.82 | 0.77 | 0.72 |
| $\epsilon_{\text{coh,HF}}$ | 0.32 | -0.16 | -0.15 | -0.12 | -0.26 |
| $\epsilon_{\text{coh,expt}}$ | -1.58 | -1.13 | -0.98 | -0.82 | -0.82 |

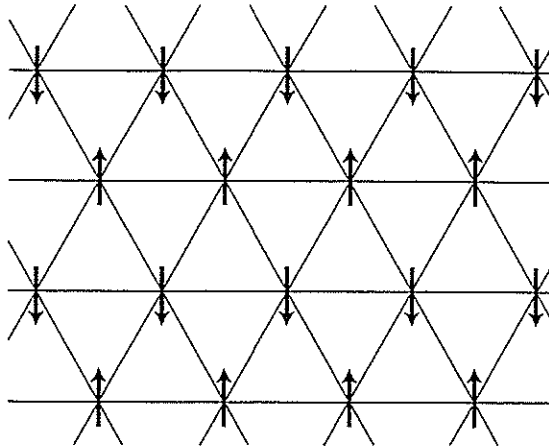


Fig. 6.2

A two-dimensional (2d) Wigner lattice of electrons. For $d = 2$, a triangular lattice minimizes the $1/r$ Coulomb repulsion between the electrons. The arrows on each lattice site reflect the orientation of the electron spin. Because a triangular lattice is not bipartite, i.e., it cannot be split into two equivalent sublattices, it does not support long-range antiferromagnetic order. Monte Carlo calculations (TC1989) indicate that for $r_s > 37$, a transition to a Wigner solid occurs with the spin configuration shown here. Wigner solid formation has been observed for electrons on the surface of liquid helium (G1979), as well in a dilute hole gas (Y1999) confined to move at the interface between GaAs and AlGaAs. In the presence of an external magnetic field, the Wigner crystal should be stable at higher densities, since a magnetic field tends to freeze out the electron zero-point motion. Experiments on a dilute 2d electron gas in a large perpendicular magnetic field (S1992) also confirm the formation of a Wigner crystal.

As is evident, while the Hartree–Fock approximation predicts that atoms in a metal are bound, it does not give accurate quantitative predictions. In fact, the non-interacting picture, $\epsilon_{\text{coh,NI}}$, did much better. To improve the theory, we need to include higher order electron–electron interactions, i.e., we need to determine more precisely the effect of correlations on the energy for a many-body system.

6.3.2 Wigner solid

Wigner’s interpolation scheme (W1934), in which he treats the system at high densities ($r_s \rightarrow 0$) perturbatively and at low densities ($r_s \rightarrow \infty$) as a solid, is more directly applicable to calculating the effect of correlations on the energy of the electron gas. Wigner’s crucial observation was that in a low-density electron gas in a uniform ion background, the electrons should form an ordered array. The 2d analog of a Wigner crystal is shown in Fig. 6.2. The basic idea is that, in this limit, the energy of the ground state, as a sum of kinetic and Coulombic terms, is dominated by the Coulomb repulsion, since $\epsilon_{\text{kin}} \sim 1/r_s^2$ while $\epsilon_{\text{coul}} \sim 1/r_s$, so that as $r_s \rightarrow \infty$, $\epsilon_{\text{kin}} < \epsilon_{\text{coul}}$. To minimize the Coulomb repulsion, the electrons find it energetically favorable to organize themselves in an ordered array. In three dimensions, the most favorable array is a body-centered cubic (bcc) lattice, although the face-centered array is quite close in energy; the simple cubic array is less favorable. An antiferromagnetic

bcc lattice is stable (CA1999) for $r_s > 93$. A transition to a ferromagnet (OHB1999) appears to occur around $r_s \approx 65$.

The energy of a Wigner solid is determined entirely by the Coulomb energy. To estimate the energy, we calculate the energy of a neutral Wigner-Seitz cell, this time containing an electron in its center with a uniform ion background. As earlier, the interaction energy between neutral Wigner-Seitz cells is a higher-order correction. In a spherical cell, the interaction energy between the uniform positive background and an electron localized at the center is given by

$$\epsilon_{ei} \approx -n_e e^2 \int_0^{r_e} \frac{dr}{r} = -\frac{3}{2} \frac{e^2}{r_e}. \quad (6.34)$$

The compensating positive background provides a uniform electrostatic energy that is the analog of the direct Coulomb interaction determined in the earlier discussion of the Wigner-Seitz method, Eq. (6.30), $\epsilon_{\text{direct}} \simeq 3e^2/5r_e$. The energy of the Wigner solid is then

$$\epsilon_{\text{WS}} = \left(\frac{3}{5} - \frac{3}{2} \right) \frac{e^2}{r_e} = -\frac{9}{10} \frac{e^2}{r_e} = -\frac{1.8}{r_s} \text{Ry}. \quad (6.35)$$

The contribution to the energy of a Wigner crystal from zero-point fluctuations of the electrons around their equilibrium positions falls off as $1/r_s^{3/2}$ (Problem 6.5) and need not be included in extracting a first approximation to the correlation energy.

In order to identify the correlation energy in the Wigner solid, we write

$$\epsilon_{\text{WS}} = \epsilon_{\text{exch}} + \epsilon_{\text{corr}} = \left(\frac{-0.916}{r_s} - \frac{0.884}{r_s} \right) \text{Ry}. \quad (6.36)$$

For large r_s , the correlation energy is thus

$$\epsilon_{\text{corr}} \approx -\frac{0.884}{r_s} \text{Ry}, \quad r_s \rightarrow \infty. \quad (6.37)$$

In the high-density regime, one can resort to the perturbative treatment of Gell-Mann and Brueckner (GB1957). In perturbation theory, the second-order term in the electron-electron interaction is of the form

$$E_{\text{coul}}^{(2)} = \sum_{\mu \neq 0} \frac{\langle p | V_{ee} | \mu \rangle \langle \mu | V_{ee} | 0 \rangle}{E_0 - E_\mu}, \quad (6.38)$$

where $|\mu\rangle$ is an intermediate excited state. All terms in the perturbative expansion can be represented diagrammatically, as can be shown using Wick's theorem. The second-order diagrams that enter are of the form shown in Fig. 6.3.

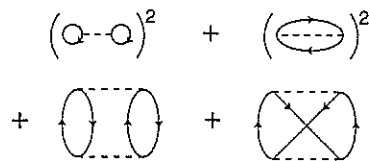


Fig. 6.3 Second-order correlation diagrams in a perturbation expansion for the ground state energy of the uniform electron gas. The solid lines indicate electrons, and the dashed lines represent the two-body Coulomb interaction.

The last diagram in Fig. 6.3, the exchange term involving just a single electron loop, is logarithmically divergent. Gell-Mann and Brueckner (GB1957) recognized that by clever resummation of a whole class of such divergent terms, they could get a finite but non-analytic result. Indeed, they found an expansion for the energy of the electron gas,

$$\epsilon_{\text{GB}} = \left(\frac{2.21}{r_s^2} - \frac{0.916}{r_s} + 0.062 \ln r_s - 0.096 + \dots \right) \text{Ry.} \quad (6.39)$$

Note the presence of the non-analytic term $\ln r_s$. This term reflects the fact that the energy of the system cannot be analytic in e^2 about $e^2 = 0$; indeed, the physics of a system of electrons with $e^2 < 0$ is that of a self-gravitating cloud, and is qualitatively different from that with $e^2 > 0$. The problem with applying perturbation theory, even in its resummed form, is that real metals lie in the region of $r_s > 1$, and hence one would have to sum the entire series to have quantitatively accurate results. It is customary to define the *correlation energy* by writing the energy of the electron system in the form

$$\epsilon = \epsilon_{\text{kin}} + \epsilon_{\text{exch}} + \epsilon_{\text{corr}}; \quad (6.40)$$

thus the Gell-Mann and Brueckner result for the correlation energy in the high-density limit is

$$\epsilon_{\text{corr}} \approx 0.062 \ln r_s - 0.096, \quad r_s \rightarrow 0. \quad (6.41)$$

Taking $\epsilon_{\text{corr}} = -0.096$ Ry at $r_s = 1$, we may write, in the spirit of Wigner, a simple approximate interpolation between the high- and low-density results:

$$\epsilon_{\text{corr}} = -\frac{0.884}{r_s + 8.21} \text{Ry} = -\frac{12.03}{r_s + 8.21} \text{eV}. \quad (6.42)$$

As Pines (P1955) has pointed out, the correlation energy at $r_s = 1$ is closer to -0.11 Ry. Nonetheless, we work within the perturbative scheme (GB1957) and use Eq. (6.42) as the interpolation formula for the correlation energy. With Eq. (6.42), we obtain the correlation and cohesive energies:

| Table 6.6 | | | | | |
|--------------------------------------|-------|-------|-------|-------|--------|
| eV | Li | Na | K | Rb | Cs |
| ϵ_{corr} | -0.7 | -1.15 | -1.07 | -1.02 | -1.17 |
| $\epsilon_{\text{coh}, W}$ | -1.64 | -1.15 | -1.02 | -0.96 | -0.92 |
| $\epsilon_{\text{coh}, \text{expt}}$ | -1.58 | -1.13 | -0.98 | -0.82 | -0.815 |

The improvement with the use of Wigner interpolation is marked.

However, while Eq. (6.42) is a useful interpolation formula for the cohesive energy, the Wigner scheme implicitly assumes that no new phases of the electron gas appear between the dense perturbative limit and the crystalline regime. There is really no basis for this assumption. In fact, one of the unsolved problems in solid state physics is what phase of matter arises when a Wigner crystal melts. As perturbation theory cannot be used at the Wigner melting boundary, this problem has no easy resolution. At the writing of this chapter, experiments on a dilute two-dimensional electron gas (K1999) indicate that this phase is exotic.

Summary

We have shown in this chapter how the Hartree-Fock procedure can be implemented in the context of the electron gas in a compensating positive background. The key result is that the eigenfunctions are plane waves, but the single-particle energy levels are lowered by the exchange interaction. The exchange interaction produces a diminished electron density around each electron. The Hartree-Fock description, however, does not describe accurately the bandwidth or the specific heat, leading to a $T/\ln T$ behavior in the latter quantity. In Chapter 9, we show how inclusion of electron screening remedies some of the failures of Hartree-Fock. To make accurate estimates of the cohesive energy of crystals, the Wigner interpolation scheme is quite successful. The underlying physics in this scheme is that at sufficiently low densities, an ordered electron lattice minimizes the energy of the electron gas. In $d = 3$, a bcc lattice is favored, while in $d = 2$, a triangular lattice of electrons forms.

Problems

6.1 Show that

$$\frac{1}{2} \int_0^{p_F} \epsilon_{\text{exch}}(\mathbf{p}) \frac{d\mathbf{p}}{(2\pi\hbar)^3} = -\frac{e^2 p_F^4}{4\pi^3 \hbar^4}.$$

6.2 Assuming the Hartree-Fock expression for the specific heat of an electron gas, $\sim T/|\ln T|$, determine the temperature for Na below which corrections to the linear specific heat would become significant (10% say).